Sensing water absorption in hygrothermally aged epoxies with terahertz time-domain spectroscopy

Hungyen Lin[1*], Benjamin P. Russell[2], Prince Bawuah[3] and J. Axel Zeitler[3]

[1]Engineering Department, Lancaster University, Gillow Avenue, Lancaster LA1 4YW, United Kingdom
[2]Experimental Materials Science, Hexcel Composites Ltd., Ickleton Road, Duxford CB22 4QB, United Kingdom
[3]Department of Chemical Engineering and Biotechnology, University of Cambridge, Philippa Fawcett Drive, Cambridge CB3 0AS, United Kingdom
*h.lin2@lancaster.ac.uk Tel: +44 (0)1524 593013

Abstract
In the field of non-destructive testing, terahertz sensing has been used to analyse a wide range of materials where the most successful applications have involved materials that are semi-transparent to terahertz radiation. In this work, we demonstrate the sensitivity of terahertz time-domain spectroscopy to quantify water absorption in hygrothermally aged simple and commercial epoxy systems supported by conventional gravimetric analysis.

Keywords: epoxy, terahertz, THz-TDS, polymer

Introduction
Epoxies represent an interesting class of materials containing reactive monomers that can cross-link either themselves or with hardners such as amines as part of the curing process. Epoxy materials have found applications as encapsulations in the electronics industry, adhesives in structural bonding, anti-corrosive protective coatings on metal structures and in the creation of composites[1].

The terahertz range of the electromagnetic spectrum (loosely between 0.1-4 THz) can provide unique insights when investigating polymers, which are semi-transparent at these frequencies. Compared to other analytical methods such as neutron and X-ray diffraction, near-infrared (NIR)[2] and microwave spectroscopy, terahertz radiation offers an interesting opportunity for materials analysis within the constraints of spatial resolution (at several hundreds micrometres) and penetration depth (up to several millimetres). Terahertz radiation is also readily accessible via table-top instruments realising terahertz time-domain spectroscopy (THz-TDS). In general, THz-TDS is an efficient technique for the coherent generation and detection of broadband terahertz radiation: a femtosecond pulsed near-infrared laser is focused onto a terahertz emitter (semiconductor photoconductive antenna or nonlinear crystal) where each optical pulse results in the excitation of sub-picosecond pulses with a bandwidth spanning from a few hundred GHz to a few THz. The emitted terahertz pulses in turn interact with the sample of interest and the resulting terahertz electric fields are measured through a coherent detection scheme either by means of photoconduction or electro-optical detection. The advantage of this approach is that the amplitude and phase of a terahertz pulse can be resolved with an excellent signal-to-noise ratio, which can be used to extract the sample's complex refractive index, an intrinsic property of the material that includes both the refractive index and absorption coefficient at the terahertz spectral range.

The advent of THz-TDS have opened up many exciting applications[3-9]. Examples of where THz-TDS has been used in polymer science and testing include detecting morphology changes and monitoring glass transition temperature[10], monitoring the polymer compounding process[11], measuring moisture content and solvent diffusion dynamics, and evaluating adhesive bonds between non-absorbing materials[12]. For epoxies in particular, THz–TDS has been used as part of standard characterisation[13] and monitoring the degree of cure[14,15]. However, there is no report on investigating water uptake of epoxies with THz-TDS. This is important because water exposure can cause a loss in physical properties such as swelling, hydrolysis, lowering of the glass transition temperature, cracking, and crazing. The extent of water uptake, however, depends on the chemistry of the network being formed[16,17], the cure temperature[18,19] and the presence of fillers[20]. In this investigation, we demonstrate the sensitivity of THz-TDS to quantify water absorption hygrothermally aged epoxy systems, for both simple and commercial systems, supported by conventional gravimetric analysis.

Materials and methods

Materials and ageing

A total of five epoxy systems were used for this study: two commercial systems with the names 8552 and RMT6, and 3 simple systems comprising the same epoxy (Epikote 828) and amine (Jeffamine T403) at 3 different stoichiometries (S060, S100, S180) where the number after the “S” refers to the proportion of reactive hydrogen sites as a percentage of the available epoxy ring sites. The process of making the simple systems were:

1. Weighing out liquid epoxy monomer and amine (combined mass of 150 g using balance with precision ±0.01 g)
2. Mixing: 120 seconds at 1000 RPM
3. Degassing under vacuum for 2-3 hours
4. Mould was filled and cured at room temperature for 3 days followed by a post-cure at 70°C for 16 h

This process was slightly different for the commercial systems. In particular, premixed resin and curative were weighted and mould was subsequently filled and cured at 180°C for 120 min (for both 8552 and RTM6). Each epoxy system was first manufactured into plaques and disc-shaped samples were cut-out from the plaques by a water-jet cutting process (Mach 3B series, Hinckley, UK), measuring 13 mm in diameter with a nominal thickness of 2 mm. For each of the five epoxy specimens investigated, there were three repeats. To ensure unique identification of the samples, engravings were made onto the sample edges prior to ageing as this was found to be a robust method to encode sample IDs for express identification thereafter. Prior to any moisture exposure, all samples underwent a drying procedure, where the samples were placed in an oven at 70°C for 200 h and on removal, they were packaged into airtight containers with desiccant.

Terahertz time-domain spectroscopy

The hygrothermal conditions provide means to the accelerated aging. In particular, this was performed by immersing the samples, held in a plastic tube with perforated holes, in distilled water in a beaker at a temperature of 95 ºC, as shown in Figure 1a. At each time increment, the samples were 1) removed from the conditioning chamber and blotted dry using a lint-free towel; 2) measured in terms of mass using an analytical balance at ±0.1 mg (Fisher Scientific, Illkirch-Graffenstaden, France), thickness using a micrometer ±1 µm (Sealey Digital External

Micrometre 0-25mm; Rapid Electronics Limited, Colchester, UK) and THz-TDS; 3) returned to conditioning chamber where the time between measurement and immersion was approximately 12 minutes. The duration of the ageing experiment was 80 h in total. The measurement of the samples at time, t = 0, corresponds to the dry epoxy discs prior to ageing. In the initial period, in order to track rapid changes of ageing, measurements were performed at 1 h intervals for the first four hours of ageing followed by a 2 h and a 3 h sampling intervals for the first day. Following an interval of approximately 10 h between the first and the second day, subsequent measurements on the second day were mostly performed at 5 h interval and followed by increasingly large time intervals until the end of the experiment. It is worth mentioning that the water level in the beaker, at any time, was kept at near constant level to ensure the samples were kept fully submerged throughout the ageing time. This was achieved by refilling the beaker at set given time intervals during the ageing process.

We performed transmission terahertz spectroscopy using a commercial THz-TDS setup (Terapulse 4000, TeraView Ltd., Cambridge, UK) shown in Figure 1c. For the measurements we selected the high-resolution scanning mode with 20 waveform averages, which took approximately 40 s per measurement. Given the sharp and distinct absorption features due to the rotational transitions of water molecules in the gas phase, all terahertz measurements were performed under a continuous purge with dry nitrogen in the sample chamber of the spectrometer. As a standard routine to all our measurements, a reference measurement was always acquired without the sample being present and taken immediately before the sample measurement to remove potential baseline drift effects. The acquired waveform of the terahertz electric field for both the sample and the reference were then converted to the frequency-domain by fast Fourier transformation. By normalising the sample spectra against the reference spectra, a complex-valued transmission function that contains both the amplitude and the phase of the transmission spectra can be determined. The frequency dependent refractive index and absorption coefficient of the samples can then be calculated from the measured phase and amplitude using Equations (1) and (2)

$$n(v) = 1 + \frac{c}{2\pi v d}\varphi(v) \tag{1}$$

$$a(v) = -\frac{2}{d} ln\left[t(v)\frac{(n(v)+1)^2}{4n(v)}\right] \tag{2}$$

where v is frequency, $t(v)$ is the complex ratio between sample and reference measurement, $\varphi(v)$ is the phase difference between sample and reference, d is sample thickness and c is the speed of light in vacuum[21]. It should be noted that refractive index is extracted from the phase information only, firstly by unwrapping, a process of adding or subtracting multiples of 2π to the phase, followed by corrections where the unreliable low-frequency phase values are discarded and replaced with a low-frequency extrapolation down to DC frequencies phases based on the reliable phase measurements at higher frequencies. A detailed mathematical description of the steps can be found elsewhere[22,23]. These relations in turn can be converted to the complex relative permittivity $\tilde{\varepsilon}(v) = \varepsilon'(v) - j\varepsilon''(v)$, commonly used in dielectric measurements, with real and imaginary parts given by Equations (3) and (4), respectively

$$\varepsilon'(v) = n^2(v) - \left(\frac{a(v)c}{4\pi v}\right)^2 \tag{3}$$

$$\varepsilon''(v) = 2n(v)\left(\frac{a(v)c}{4\pi v}\right) \quad (4)$$

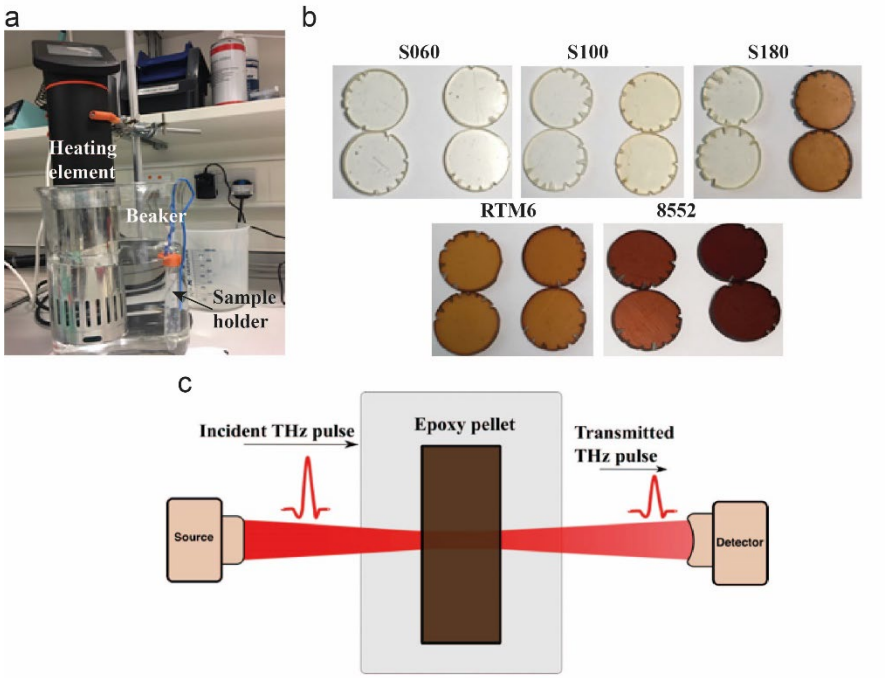

Figure 1. Water heating setup a) used to hygrothermally age the epoxy samples, where colouration was observed before (left) and after (right) conditioning b). These samples were measured using THz-TDS in c).

Results & discussion

Figure 1b shows that the samples all underwent distinct irreversible colour changes (yellowing) during the ageing process, with S180 being the most affected and S060 being the least. Yellowing in bulk is a well-known phenomenon in aliphatic amine cured epoxy systems, and relates to various oxidation processes in which N-H_2 groups participate[24]. The observed colour changes are most significant for the S180 specimens, which are at their greatest concentration of amines. The extracted frequency dependent refractive indices and absorption coefficients of the samples at different time increments are shown in Figure 2. It should be noted that spectral oscillations observed at frequencies higher than 1.5 THz are due to noise, approaching system's dynamic range[21]. As expected, the amorphous morphology of the epoxy materials results in featureless, monotonically increasing absorption spectra, with the refractive index spectra decreasing with increasing frequency[13]. Considering that the amine and epoxies are both polar molecules, it was expected that the cross link density would be highest when epoxy and amine concentration was equal (S100). This hypothesis appears to be valid from Figure 3, where S100 does exhibit the highest mass. It is, however, not evident in the refractive index, a measure of material's optical density, where specimen S060, with the lowest amine concentration, actually exhibited the highest refractive index. For the spectrometer used and the thickness of the samples chosen for our experiments we found that the useable bandwidth was approximately from 0.4 to 1.5 THz. Diffusion of water into cured epoxies is generally thought to obey Fick's second law in one dimension[25], which is described as

$$\frac{dC}{dt} = D\frac{d^2C}{dx^2} \tag{5}$$

where C is the concentration, t is time, x is the position and D is the diffusion coefficient. The diffusion coefficient in turn can be determined from the initial gradient of the sorption curve obtained by plotting the change in mass against the square root of time divided by the thickness[26], as shown in Table 1. For comparison against gravimetric measurements, Figure 3 shows the refractive index and absorption coefficient at 1 THz as a function of water ageing time. Even though 1 THz is used to represent the spectra, in principle other frequencies across the usable bandwidth could also be used, which either would shift the absorption coefficient curves vertically up or the refractive index curves down. The similarity of the curves, nevertheless, would remain approximately the same. Pearson correlation coefficients between the respective curves are shown in Table 2 and generally take values greater than 0.95, thus suggesting a strong linear correlation between the measured terahertz optical constants and the gravimetric measurement.

Table 1– Diffusion coefficient of the epoxy systems

Epoxy system	Diffusion coefficient ($mm^2s^{-1)}$
S060	$8.633x10^{-6}$
S100	$2.69\ x10^{-5}$
S180	$6.75\ x10^{-5}$
RTM6	$1.523\ x10^{-5}$
8552	$5.942x10^{-6}$

The dielectric properties of materials with different water content can be described by using the methods of effective medium theory (EMTs). Such treatments make it possible to calculate macroscopic permittivity at terahertz frequencies as a function of water content. Here, we describe the mixture of water and epoxy resin using the Landau, Lifshitz, Looyenga (LLL) model[27], which assumes a virtual sphere that includes particles of a given volumetric fraction and of arbitrary shapes. By successively adding an infinitesimal amount of particles, the effective permittivity is increased slightly and can be described by a Taylor approximation. As there is no particle shape dependency, the model can be applied to irregularly shaped particle mixtures and has been used successfully to quantify water content inside polymers and plant leaves[28,29]. It should be noted that whilst the LLL model was initially proposed for two components mixtures, the model can be extended to three components to account for additional contributions such as free water in a higher water absorbing polymers or the air pockets inside a plant leaf. The complex permittivity of aged epoxy $\tilde{\varepsilon}_k(v)$ can be described as

$$\sqrt[3]{\tilde{\varepsilon}_k(v)} = f_{\mathrm{BW},k}\sqrt[3]{\tilde{\varepsilon}_{\mathrm{BW}}(v)} + \left(1 - f_{\mathrm{BW},k}\right)\sqrt[3]{\tilde{\varepsilon}_{\mathrm{D}}(v)} \tag{6}$$

where $\tilde{\varepsilon}_{\mathrm{BW}}(v)$ is the complex permittivity of bound water, $\tilde{\varepsilon}_{\mathrm{D}}(v)$ is the complex permittivity of the dry epoxy. Both permittivities are weighted by their respective volumetric fractions $f_{\mathrm{BW},k}$ and $1 - f_{\mathrm{BW},k}$ for a two component mixture where the sum of the volumetric fractions is one. The volumetric fraction $f_{\mathrm{BW},k}$ is determined by the following relation

$$f_{\mathrm{BW},k} = \frac{m_k - m_0}{\rho A d_k} \quad (7)$$

where m_k is the mass of aged epoxy at time k, m_0 is the mass of dry epoxy before conditioning, ρ is the density of water taken as 1 g.cm^{-3}, and A is the sample area. Bound water here refers to the polar water molecules that bind to the polar functional groups of the epoxy macromolecules by means of intermolecular hydrogen bonds. The vibrations of the bound water molecules, as shown previously in polymers, such as polyamide and wood plastic composites[29], differ to that of the free water, which is characterised by double Debye relaxation processes[30]. The LLL model in Equation (6) additionally requires an estimation of the bound water permittivity, which is approximated to be the average of the permittivities at time increments between 2 to 5 hours. Even though the number of time increments can be extended, it would not result in significant improvement to fitting to the measurement. The method of determining the bound water permittivity by averaging out initial permittivity values is a similar approach to what was taken previously where the average between second to the tenth day of measurements was used[29]. Noticeably, the number of data points needed here is significantly less due to the accelerated ageing applied as well as the different specimens studied. Contributions from the respective components are then weighed by the volumetric fraction determined from the gravimetric measurements in order to estimate the complex permittivity of aged epoxy.

Using Equations (1-4), the raw data were processed and Figure 4 shows plots of the refractive index and absorption coefficients at 1 THz from the measurements as well as the results from the LLL model as a function of water uptake. The data are presented across the different epoxy systems for all samples, and generally the model is able to achieve a good fit to the data. Notable exceptions include samples S060 and S180, where the LLL model fails altogether, after 2 and 4 % of water uptake, respectively. This means that the measured complex permittivity can no longer be considered a straight-forward ideal mixture of dry and bound water epoxy, but that the dielectric responses of the constituent phases have changed, which is likely to be due to chemical changes in the epoxy material. The exact cause, however, is unclear given the complex nature of the chemical changes that take place during hygrothermal conditions as well as the different epoxy formulations used. At the same time, the observed changes are somewhat unsurprising because the stoichiometries used in these specimens were entirely artificial and extreme. In the case of S180, physical changes such as sample disintegrations and the associated weight loss were noted. In contrast for S060, samples became noticeably softer. These physical changes could be due to various irreversible processes that occured during the hygrothermal ageing process, such as hydrolysis, thermo-oxidation and leaching[24], and is the subject of future investigations. For the specimens where a good agreement between measurement and modelling were observed, such as the commercially relevant RTM6 and 8552, the results from our terahertz measurements suggest that there is a possibility to estimate water content inside an aged epoxy specimen without conventional gravimetric measurement. Instead, water content can be estimated by performing a single terahertz point measurement on the sample and carrying out the aforementioned analysis thereafter using the permittivity and water uptake plots, such as in Figure 4, for calibrations.

Considering the measurement error bars, the results also suggest that absorption coefficient is perhaps a more robust measure than refractive index where measuring the sample

thickness accurately becomes notably more difficult when the samples softens inherently as part of the ageing process. Compared to conventional gravimetric measurement and dielectric spectroscopy, the proposed measurement does not require physical contact to the sample and operates at a spatial resolution of several hundreds of micrometres thus enabling water spatial distribution to be imaged.

Table 2– Pearson correlation coefficients between gravimetric analysis and refractive index and absorption coefficient at 1 THz as function of ageing time

Epoxy system	Correlation coefficient (refractive index)	Correlation coefficient (absorption coefficient)
S060	0.951	0.9157
S100	0.9874	0.9961
S180	0.9660	0.9684
RTM6	0.9832	0.9848
8552	0.9835	0.9974

Conclusion

In this study, we have demonstrated the sensitivity of THz-TDS to resolve water absorption during a hygrothermal ageing process, in a total of five different epoxy systems (two commercial and three simple with increasing amine concentration), benchmarked by conventional gravimetric analysis. Using EMT in the form of the LLL model, the bound water uptake can be quantified at sufficient fidelity across epoxy systems where epoxy and amine concentration was equal. Without a loss of generality, the presented methodology can also be applied to other epoxy systems provided that they are semi-transparent to terahertz radiation. Our data shows that while measurement and analysis are understandably more complex, compared to conventional gravimetric analysis, THz-TDS is a highly interesting contactless, quantitative characterisation technique with clear potential to complement existing characterisation techniques and to open up new opportunities for future rapid and accelerated degradation testing.

Acknowledgements

H.L. acknowledge financial support from the EPSRC (Grant No. EP/R019460/1, H2FC Supergen Flexible Grant EP/P024807/1, and UK EPSRC Teranet Seedcorn Fund EP/M00306X/1). The authors acknowledge Ms Coralie Chasse for sample preparation, Dr Mira Naftaly at National Physical Laboratory, UK for initial discussions.

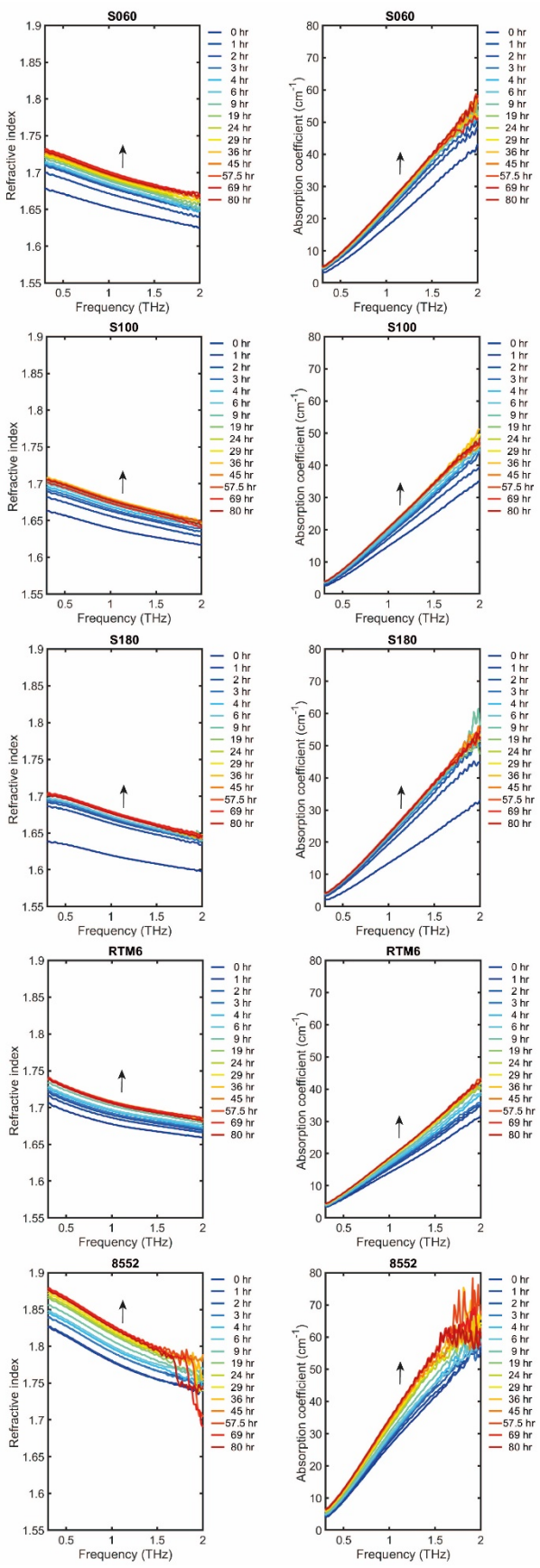

Figure 2 – Terahertz refractive index and absorption coefficient of the specimens at different water ageing time.

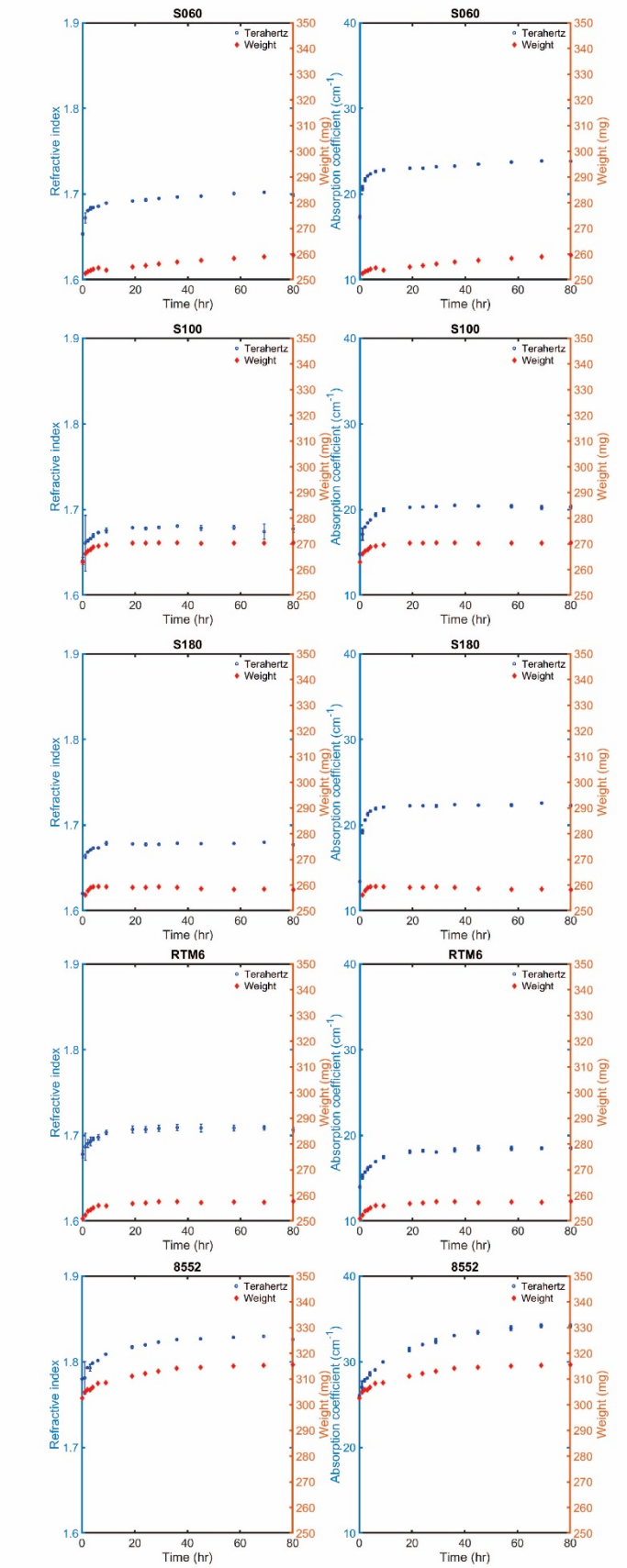

Figure 3 – Refractive index and absorption coefficient at 1 THz together with gravimetric measurements as a function of water ageing time.

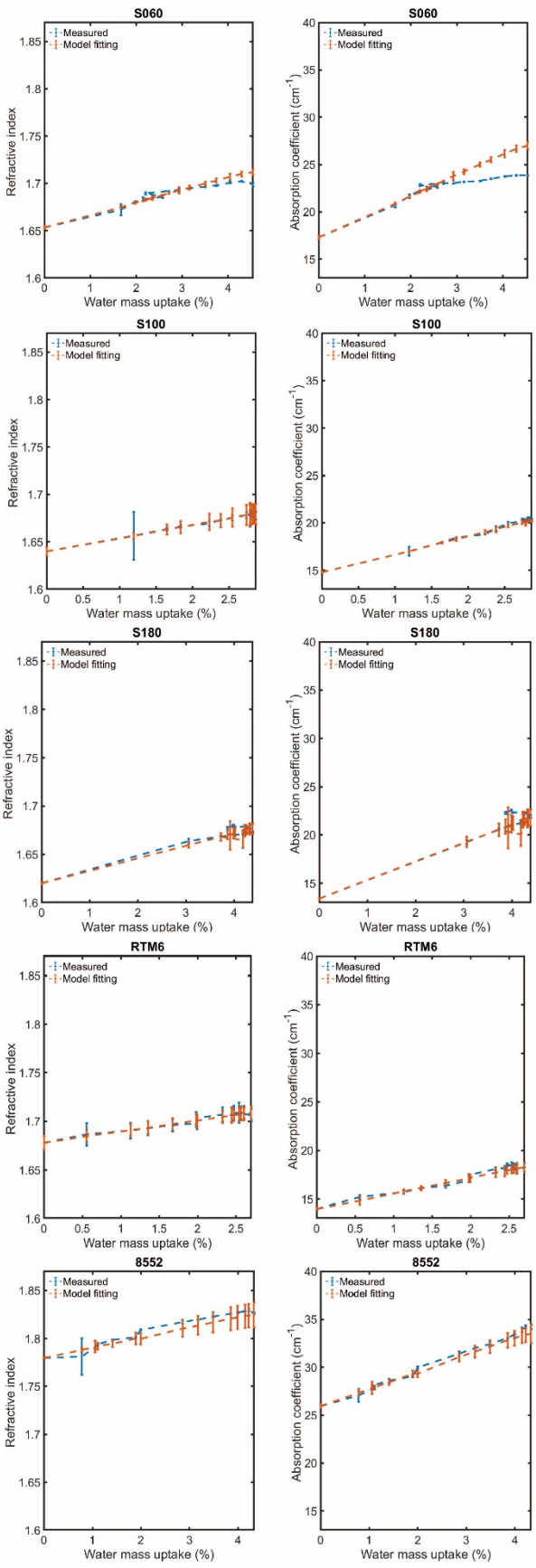

Figure 4 – Refractive index and absorption coefficients at 1 THz from measurement and estimated using LLL model as a function of water uptake. Lines are plotted to guide the eye.

Contributions

All authors conceived and designed the experiments. B.P.R. prepared all the samples. P.B. performed all the experiments and measurements. H.L., B.P.R. and P.B. performed analysis. All authors interpreted the results. H.L., B.P.R. and P.B. wrote the main manuscript and prepared the figures. All authors reviewed the manuscript. H.L. and B.P.R. secured funding for this research.

Competing interests

The authors declare no competing financial interests.

Data availability

Additional data sets related to this publication are available from the Lancaster University data repository.

References

(1) Pethrick, R. A. *Polymer science and technology for scientists and engineers*; Whittles: Dunbeath, Scotland, Hoboken, NJ, 2010, p xvi, 360 p.
(2) Fyfe, C. A.; Randall, L. H.; Burlinson, N. E. *J Polym Sci Pol Chem* **1993**, *31*, 159-168.
(3) Lin, H.; Braeuninger-Weimer, P.; Kamboj, V. S.; Jessop, D. S.; Degl'Innocenti, R.; Beere, H. E.; Ritchie, D. A.; Zeitler, J. A.; Hofmann, S. *Sci Rep-Uk* **2017**, *7*.
(4) Lin, H.; Burton, O. J.; Engelbrecht, S.; Tybussek, K.; Fischer, B. M.; Hofmann, S. *Applied Physics Letters* **2020**, *116*, 021105.
(5) Lin, H.; May, R. K.; Evans, M. J.; Zhong, S. C.; Gladden, L. F.; Shen, Y. C.; Zeitler, J. A. *J Pharm Sci-Us* **2015**, *104*, 2513-2522.
(6) Naftaly, M.; Vieweg, N.; Deninger, A. *Sensors-Basel* **2019**, *19*.
(7) Vynckier, A. K.; Lin, H.; Zeitler, J. A.; Willart, J. F.; Bongaers, E.; Voorspoels, J.; Remon, J. P.; Vervaet, C. *Eur J Pharm Biopharm* **2015**, *96*, 125-131.
(8) Yassin, S.; Su, K.; Lin, H.; Gladden, L. F.; Zeitler, J. A. *J Pharm Sci-Us* **2015**, *104*, 1658-1667.
(9) Yu, C.; Fan, S.; Sun, Y.; Pickwell-Macpherson, E. *Quantitative imaging in medicine and surgery* **2012**, *2*, 33-45.
(10) Wietzke, S.; Jansen, C.; Reuter, M.; Jung, T.; Kraft, D.; Chatterjee, S.; Fischer, B. M.; Koch, M. *J Mol Struct* **2011**, *1006*, 41-51.
(11) Scheller, M.; Wietzke, S.; Jansen, C.; Koch, M. *J Phys D Appl Phys* **2009**, *42*.
(12) Jansen, C.; Wietzke, S.; Wang, H. Y.; Koch, M.; Zhao, G. Z. *Polym Test* **2011**, *30*, 150-154.
(13) Stubling, E.; Gomell, L.; Sommer, S.; Winkel, A.; Kahlmeyer, M.; Bohm, S.; Koch, M. *J Infrared Millim Te* **2018**, *39*, 586-593.
(14) Probst, T.; Sommer, S.; Soltani, A.; Kraus, E.; Baudrit, B.; Town, G. E.; Koch, M. *J Infrared Millim Te* **2015**, *36*, 569-577.
(15) Sommer, S.; Probst, T.; Kraus, E.; Baudrit, B.; Town, G. E.; Koc, M. *Polym Sci Ser B+* **2016**, *58*, 769-776.
(16) Hayward, D.; Hollins, E.; Johncock, P.; McEwan, I.; Pethrick, R. A.; Pollock, E. A. *Polymer* **1997**, *38*, 1151-1168.
(17) Li, L.; Yu, Y. F.; Wu, Q. L.; Zhan, G. Z.; Li, S. J. *Corros Sci* **2009**, *51*, 3000-3006.
(18) Grave, C.; McEwan, I.; Pethrick, R. A. *J Appl Polym Sci* **1998**, *69*, 2369-2376.
(19) Johncock, P.; Tudgey, G. F. *Brit Polym J* **1986**, *18*, 292-302.
(20) Aronhime, M. T.; Peng, X.; Gillham, J. K.; Small, R. D. *J Appl Polym Sci* **1986**, *32*, 3589-3626.
(21) Jepsen, P. U.; Fischer, B. M. *Opt Lett* **2005**, *30*, 29-31.
(22) Scheller, M. *J Infrared Millim Te* **2014**, *35*, 638-648.
(23) Withayachumnankul, W.; Naftaly, M. *J Infrared Millim Te* **2014**, *35*, 610-637.
(24) Krauklis, A. E.; Echtermeyer, A. T. *Polymers-Basel* **2018**, *10*.
(25) Crank, J.; Park, G. S. *Diffusion in polymers*; Academic Press: London, New York,, 1968, p xii, 452 p.
(26) Garden, L.; Pethrick, R. A. *J Appl Polym Sci* **2017**, *134*.

(27) Looyenga, H. *Physica* **1965**, *31*, 401-406.
(28) Jordens, C.; Scheller, M.; Breitenstein, B.; Selmar, D.; Koch, M. *J Biol Phys* **2009**, *35*, 255-264.
(29) Jordens, C.; Wietzke, S.; Scheller, M.; Koch, M. *Polym Test* **2010**, *29*, 209-215.
(30) Kindt, J. T.; Schmuttenmaer, C. A. *J Phys Chem-Us* **1996**, *100*, 10373-10379.

For Table of Contents Only